

Colony stimulating factor 1 receptor inhibition delays recurrence of glioblastoma after radiation by altering myeloid cell recruitment and polarization

Jason H. Stafford, Takahisa Hirai, Lei Deng, Sophia B. Chernikova, Kimiko Urata, Brian L. West, and J. Martin Brown

Department of Radiation Oncology, Stanford University School of Medicine, Stanford, California (J.H.S., T.H., L.D., S.B.C., K.U., J.M.B.), Department of Radiation Oncology, Juntendo University School of Medicine, Tokyo, Japan (T.H.); Plexikon Inc., Berkeley, California (B.L.W.)

Corresponding Author: J. Martin Brown, PhD, FASTRO, Department Radiation Oncology, Div. of Radiation and Cancer Biology, Stanford University School of Medicine, 1050 Arastradero Rd, Rm A246, Palo Alto, CA 94304 (m.brown@stanford.edu).

Background. Glioblastoma (GBM) may initially respond to treatment with ionizing radiation (IR), but the prognosis remains extremely poor because the tumors invariably recur. Using animal models, we previously showed that inhibiting stromal cell–derived factor 1 signaling can prevent or delay GBM recurrence by blocking IR-induced recruitment of myeloid cells, specifically monocytes that give rise to tumor-associated macrophages. The present study was aimed at determining if inhibiting colony stimulating factor 1 (CSF-1) signaling could be used as an alternative strategy to target pro-tumorigenic myeloid cells recruited to irradiated GBM.

Methods. To inhibit CSF-1 signaling in myeloid cells, we used PLX3397, a small molecule that potently inhibits the tyrosine kinase activity of the CSF-1 receptor (CSF-1R). Combined IR and PLX3397 therapy was compared with IR alone using 2 different human GBM intracranial xenograft models.

Results. GBM xenografts treated with IR upregulated CSF-1R ligand expression and increased the number of CD11b+ myeloid-derived cells in the tumors. Treatment with PLX3397 both depleted CD11b+ cells and potentiated the response of the intracranial tumors to IR. Median survival was significantly longer for mice receiving combined therapy versus IR alone. Analysis of myeloid cell differentiation markers indicated that CSF-1R inhibition prevented IR-recruited monocyte cells from differentiating into immunosuppressive, pro-angiogenic tumor-associated macrophages.

Conclusion. CSF-1R inhibition may be a promising strategy to improve GBM response to radiotherapy.

Keywords: angiogenesis, CSF-1, glioblastoma, macrophages, radiation.

Glioblastoma (GBM) is the most common and most aggressive primary brain tumor, with median survival of <15 months after diagnosis and 2-year survival of only 25%.^{1,2} This dire prognosis is primarily due to the rapid recurrence of GBM following standard therapy, which currently consists of a combination of surgery, radiotherapy, and temozolomide chemotherapy.

Radiation therapy is an integral component of GBM treatment, and a considerable amount of effort has gone into enhancing its efficacy. Radiosensitizers, high-dose boost stereotactic radiosurgery techniques, and adjuvant therapies such as angiogenesis inhibition have all been used in an attempt to improve local control of GBM by ionizing radiation (IR).^{2–4} However, these strategies

have met with little success, and the tumors invariably recur—usually within the radiation field.⁵ Thus, there remains a pressing need to develop novel treatments that significantly enhance the efficacy of radiotherapy and are capable of preventing tumor recurrence.

Stromal cells within the tumor microenvironment, and in particular tumor-associated macrophages (TAMs), have been demonstrated to play a key role in solid tumor progression and resistance to therapy.⁶ We have previously shown in rodent models that GBM resistance to radiation is dependent on myeloid cells, specifically bone marrow–derived monocytes that give rise to TAMs, which stimulate the growth of new tumor blood vessels.⁷ The irradiated tumors secrete the chemokine

Received 23 February 2015; accepted 4 October 2015

© The Author(s) 2015. Published by Oxford University Press on behalf of the Society for Neuro-Oncology. All rights reserved.
For permissions, please e-mail: journals.permissions@oup.com.

stromal cell–derived factor 1 (SDF-1, aka CXCL12), which binds to its receptor CXCR4 expressed on circulating monocytes. Drugs that target SDF-1 or CXCR4 inhibit monocyte infiltration into tumors and delay and, in some cases, completely block GBM recurrence.^{7,8} However, other chemokines secreted by tumors have been implicated in the recruitment of pro-tumorigenic TAMs and their monocytic precursors.^{9,10}

Colony stimulating factor 1 (CSF-1) is another chemokine that appears to be a promising target for inhibiting TAM contribution to tumor progression. CSF-1 is a potent chemoattractant and is considered the most important growth factor regulating the differentiation of monocytes into macrophages.⁹ Consistent with this, CSF-1 overexpression correlates with increased TAM infiltration and poor clinical outcome in multiple types of cancer.^{9,11–14}

Here we show that inhibition of CSF-1 receptor (CSF-1R) enhances irradiation by altering both the recruitment and the phenotype of myeloid-derived cells recruited to irradiated GBM tumors. We used 2 different GBM models: luciferase-expressing U251 (U251-luc) tumors that allowed *in vivo* imaging of tumor growth and patient-derived GBM12 tumors that may have enhanced clinical relevance.¹⁵ GBM xenografts treated with IR upregulated expression of CSF-1R ligands and increased the numbers of intratumor CD11b+ myeloid cells. Treatment with the CSF-1R inhibitor PLX3397 depleted CD11b+ cells and significantly delayed recurrence of intracranial GBM tumors growing in mice treated with whole-brain irradiation (WBI). Analysis of myeloid cell differentiation markers suggested that CSF-1R inhibition also blocked IR-recruited monocytes from differentiating into immunosuppressive, pro-angiogenic TAMs.

Materials and Methods

Cell Culture

U251 human glioblastoma cells were obtained from R. K. Puri (FDA) and maintained in Dulbecco's modified Eagle's medium with 10% fetal bovine serum (Gibco). U251-luc cells were generated using the pFB-Luciferase retrovirus system (Stratagene) as previously described.⁷ GBM12 tumors were obtained from J. N. Sarkaria (Mayo Clinic) and propagated by serial transplantation in the flanks of athymic nu/nu (nude) mice (National Cancer Institute). Prior to intracranial implantation, GBM12 cells were harvested from flank tumors and grown as short-term explant cultures on Matrigel-coated flasks in Dulbecco's modified Eagle's medium with 2.5% fetal bovine serum as previously described.¹⁵

GBM Tumor Models

Subcutaneous tumors were generated by inoculating 2×10^6 U251-luc tumor cells into the left hind limb of nude mice. Orthotopic tumors were generated by intracranial inoculation of GBM tumor cells as previously described.¹⁶ Briefly, the cells were stereotactically injected into the right hemisphere of the brain at 1.5 mm posterior of the bregma, 1.5 mm to the right of the sagittal suture, and 2.5 mm below the surface of the skull. For U251-luc orthotopic tumors, 1×10^6 cells were inoculated, whereas 3×10^5 cells were inoculated for GBM12 orthotopic tumors. All tumor cells were obtained according to Stanford

University's institutional review board guidelines, and all animal procedures were approved by the Administrative Panel on Laboratory Animal Care.

Imaging and Irradiation

Growth of orthotopic U251-luc tumors was monitored by bioluminescence imaging (BLI). Mice were anesthetized with isoflurane and injected intraperitoneally with 150 mg/kg D-luciferin (PerkinElmer). The mice were imaged 5 min after injection with an IVIS Lumina imaging system (Xenogen). When the tumors reached a size corresponding to a BLI signal of $2–5 \times 10^8$ photons/sec they were given 12 Gy WBI, by using opposed lateral fields. Custom-made lead jigs were used for shielding nontarget tissues, including the buccal mucosa. WBI, subcutaneous tumor irradiation, and irradiation of cells growing in culture were performed in single fractions with a Phillips X-ray unit operated at 200 kVp with a dose rate of 1.21 Gy/min (20 mA with added filtration of 0.5 mm copper, distance from X-ray source to the target of 31 cm, and a half value layer of 1.3 mm copper).

Quantitative PCR Analysis

GBM cells growing in culture were trypsinized prior to RNA isolation. Subcutaneous tumors were harvested and pieces $\sim 3 \text{ mm}^3$ in size were disrupted with a PowerGen 125 rotor-stator homogenizer (Fisher Scientific). Myeloid cells were isolated from enzyme-digested tumors (as described for fluorescence activated cell sorting [FACS] analysis below) using an EasySep Mouse CD11b+ Selection Kit (Stem Cell Technologies). Total RNA was isolated using an RNeasy Mini Kit (Qiagen) and cDNA was synthesized using an RT² First Strand Kit (Qiagen). Real-time PCR was then performed with a 7900HT Fast Real-time PCR system (Applied Biosystems) using RT² SYBR Green ROX quantitative PCR Mastermix (Qiagen). QuantiTect primers for human and mouse genes of interest were also obtained from Qiagen. β -actin expression was used as an internal control, and fold change in gene expression between treatment groups was calculated using the comparative cycle threshold method.¹⁷

Western Blot Analysis

Brains from mice bearing orthotopic U251-luc tumors were imaged *ex vivo* using the IVIS Lumina imaging system, and the tumors were isolated from normal brain tissue. The tumors were homogenized in T-PER Tissue Protein Extraction Reagent (Thermo Fisher), and equal amounts of protein were subjected to sodium dodecyl sulfate–polyacrylamide gel electrophoresis under reducing conditions and then transferred to nitrocellulose membranes. The membranes were blocked with SuperBlock Blocking Buffer (Thermo Fisher) for 1 h and then incubated with rabbit anti-human CSF-1 antibody (Proteintech) or rabbit anti-human interleukin (IL)-34 (Abcam) diluted 1:1000 in blocking buffer overnight at 4°C. Primary antibodies were detected using horseradish peroxidase–conjugated goat anti-rabbit immunoglobulin G (Jackson ImmunoResearch) diluted 1:10 000 and SuperSignal West Substrate (Thermo Fisher). To determine loading efficiency, the membranes were stripped and reprobed with a rabbit anti- β -actin antibody (Abcam).

Fluorescence Activated Cell Sorting Analysis

Subcutaneous tumors were harvested and mechanically dissociated and single-cell suspensions were prepared by digestion with 200 $\mu\text{g}/\text{mL}$ Liberase DH (Roche) for 1 h at 37°C. Red blood cells were removed by incubation in red blood cell lysis buffer (eBioscience) for 10 min on ice, and dead cells were stained with a LIVE/DEAD cell viability kit (Life Technologies). Rat anti-mouse CD11b/fluorescein isothiocyanate, Ly6C-allophycocyanin, Ly6G-PerCP-Cy5.5, CD16/CD32 (Fc block) antibodies and isotype controls were obtained from BD Biosciences. Antibodies were incubated at a concentration of 1:500 in FACS buffer (Dulbecco's phosphate buffered saline, 2% bovine serum albumin, 1 mM EDTA, 0.02% NaN_3) for 30 min. The cells were washed 3 \times with FACS buffer and then analyzed with a FACScan flow cytometer (BD Biosciences).

Immunohistochemical Analysis

Frozen sections (10 μM) were prepared from brains from mice bearing orthotopic tumors. Malignant tissue was detected with standard hematoxylin and eosin (H&E) staining. Myeloid cells were identified by staining with a rat anti-mouse biotin-conjugated CD11b antibody (BD Biosciences), and TAMs were identified with a rat anti-mouse biotin-conjugated F4/80 antibody (AbD Serotec) or a rat anti-mouse CD206 antibody (Thermo

Fisher). All antibodies were diluted 1:500 in 1% bovine serum albumin with the exception of the anti-CD206 antibody, which was diluted 1:200. Stained sections were mounted in Prolong Gold antifade reagent with 4',6'-diamidino-2-phenylindole (Life Technologies) to counterstain cell nuclei.

Statistical Analysis

Statistical significance was determined by Student's *t*-test. *P*-values <.05 were considered to be statistically significant. Kaplan–Meier curves and the log-rank test were used to compare survival times between treatment groups. All calculations were performed using GraphPad Prism.

Results

Ionizing Radiation Induces Expression of CSF-1R Ligands in GBM Tumors

U251-luc tumors and GBM12 tumors were implanted subcutaneously in nude mice and irradiated with a single dose of 12 Gy. Quantitative PCR was used to assay expression of CSF-1 and IL-34, the known ligands for CSF-1R,¹⁸ at different time points after irradiation ($n = 5-6/\text{group}$). Irradiated U251-luc tumors exhibited increased expression of CSF-1 and IL-34 mRNA at

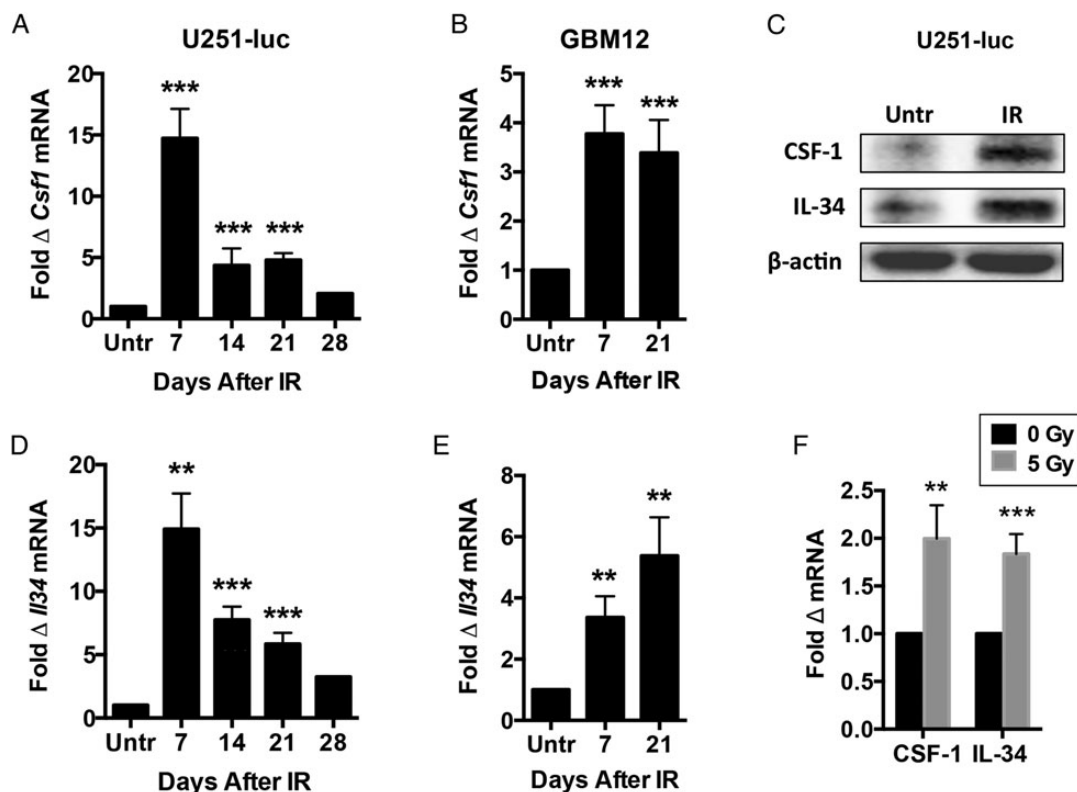


Fig. 1. IR induces expression of CSF-1R ligands in GBM tumors. Subcutaneous U251-luc (A and D) and GBM12 (B and E) tumors were irradiated with a single dose of 12 Gy and assayed for CSF-1 and IL-34 expression at different time points by quantitative (q)PCR (Untr = untreated controls). (C) Intracranial U251-luc tumors irradiated with 12 Gy were assayed for CSF-1 and IL-34 expression by western blot at 7 d after IR. (F) U251-luc cells growing in culture were irradiated with 5 Gy and analyzed by qPCR 48 h later. CSF-1 and IL-34 expression were normalized to β -actin expression in each experiment. Error bars represent mean \pm SEM for $n = 5-6$ mice or 4 culture flasks per group. *** $P < .001$ and ** $P < .01$; Student's *t*-test.

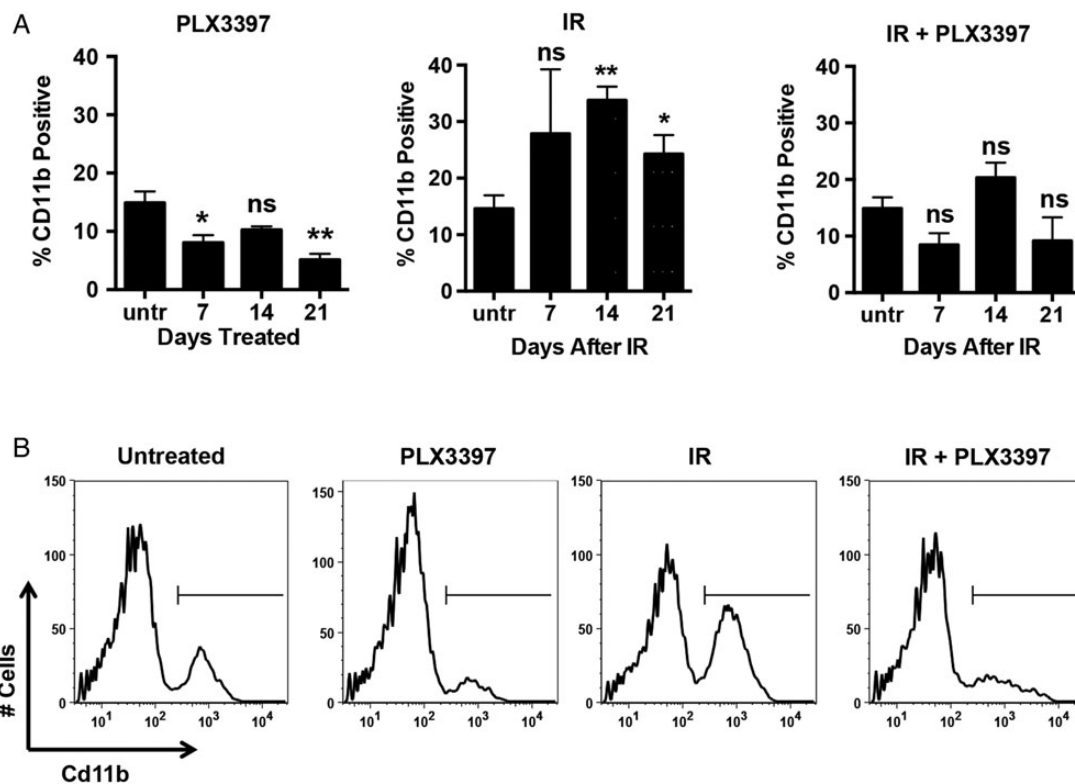


Fig. 2. CSF-1R inhibition reduces the number of CD11b+ myeloid cells in irradiated GBM tumors. Mice bearing subcutaneous U251-luc tumors were treated with PLX3397 (40 mg/kg/d), IR (12 Gy), or IR + PLX3397. (A) The tumors were harvested at different time points after irradiation and analyzed by FACS using an anti-CD11b antibody. Error bars represent mean \pm SEM for $n = 5-6$ mice. ** $P < .01$ and * $P < .05$; Student's t -test (relative to untreated). (B) Representative FACS plots from tumors analyzed at 14 d after irradiation.

all time points examined, with expression of each ligand increased more than 14-fold at 7 days after treatment compared with untreated controls and between 2- and 8-fold at later time points (Fig. 1A and D). Irradiated GBM12 tumors also showed elevated expression of CSF-1 and IL-34, with expression increased between 3- and 6-fold when examined at 7 and 21 days after treatment (Fig. 1B and E). U251-luc tumors were also implanted intracranially and assayed for CSF-1 and IL-34 protein expression by western blot 7 days after treatment with 12 Gy. Increased CSF-1 and IL-34 protein levels were detected in irradiated tumors compared with untreated controls (Fig. 1C). Finally, U251-luc cells growing in culture irradiated with 5 Gy were found to increase expression of CSF-1 and IL-34 mRNA within 48 h (Fig. 1F).

CSF-1R Inhibition Depletes CD11b+ Myeloid Cells in Irradiated GBM Tumors

Mice bearing subcutaneous U251-luc tumors were treated with PLX3397 alone (40 mg/kg/d), IR alone (12 Gy), or IR + PLX3397. Untreated controls and the "IR alone" group were given an inactive PLX3397 analog. The tumors were harvested at different time points ($n = 5-6$ /group) and analyzed by FACS using a CD11b antibody to identify myeloid-derived cells. Radiation-induced myeloid cell recruitment was highest at 14 days after treatment, with 33.7% of the cells in IR-treated tumors staining positive for CD11b compared with 14.9% in untreated controls

(Fig. 2A and B). However, only 20.2% of the cells in tumors treated with IR + PLX3397 were positive for CD11b at 14 days after treatment, which was similar to untreated controls. Tumors treated with PLX3397 alone had fewer myeloid cells at 7 and 21 days than untreated controls, but the difference between the 2 groups was not statistically significant at 14 days ($P = .06$).

CSF-1R Inhibition Sensitizes GBM Tumors to Irradiation

U251-luc tumors were implanted orthotopically into the brains of mice, and tumor growth was monitored by BLI. At 18 days after implantation, the mice were treated with PLX3397 alone, IR alone, or IR + PLX3397 ($n = 5-6$ /group). Untreated controls and the IR alone group were again given the inactive PLX3397 analog. At 50 days, BLI signals were ~ 100 -fold smaller in mice receiving IR + PLX3397 treatment than in those receiving only IR or PLX3397 alone, reflecting a large difference in tumor size (Fig. 3A and B). Median survival of mice bearing intracranial U251-luc tumors treated with IR and PLX3397 was significantly longer than that for mice treated with IR alone (87 d vs 57 d, $P < .0001$; log-rank test) and was more than twice that of untreated controls (42 d) (Fig. 3C). Median survival for mice treated with PLX3397 alone at 48 days was longer than that for untreated controls, but the difference was not statistically significant ($P = .054$).

CSF-1R inhibition also enhanced the effect of IR on orthotopic GBM12 tumors. GBM12 tumors grew at a faster rate

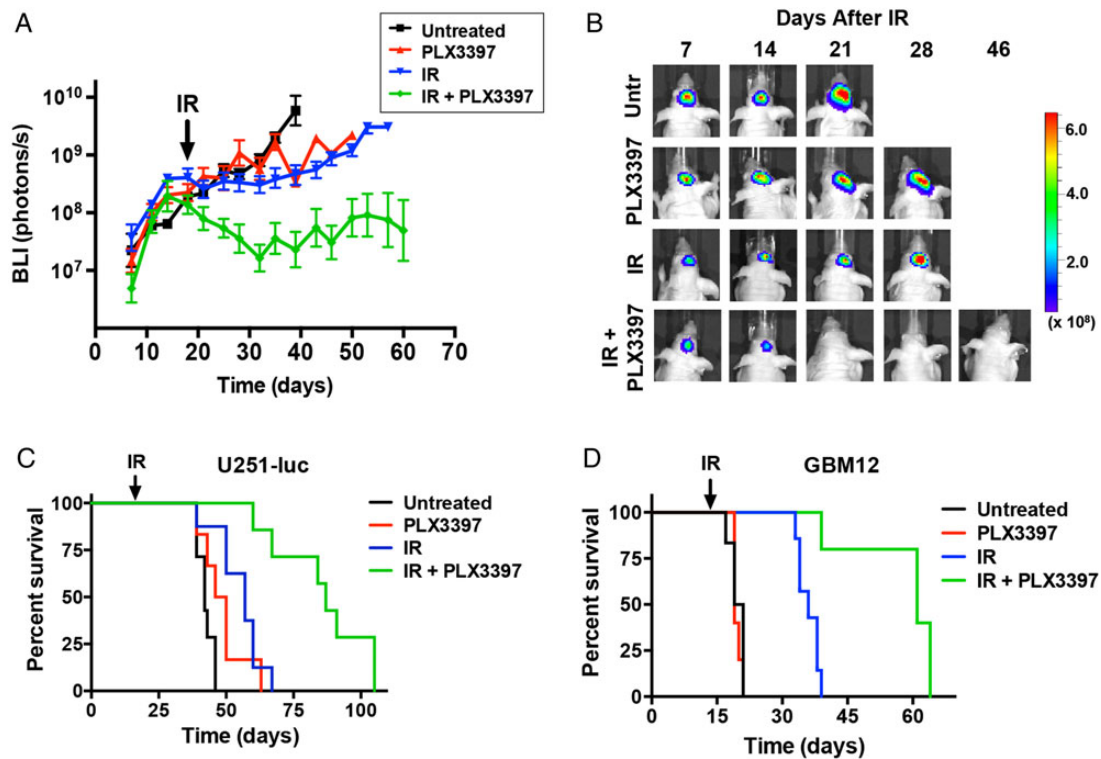


Fig. 3. CSF-1R inhibition sensitizes GBM tumors to irradiation. Mice bearing intracranial U251-luc or GBM12 tumors were treated with PLX3397 (40 mg/kg/d), IR (12 Gy), or IR + PLX3397. (A) Growth curves of intracranial U251-luc tumors measured by BLI. Error bars represent mean \pm SEM for $n = 5-6$ mice. (B) Representative BLI images showing U251-luc tumor growth in individual mice from the different treatment groups. (C) Kaplan-Meier survival curves for mice bearing intracranial U251-luc tumors ($n = 6-8$ mice/group). Median survival for mice treated with IR + PLX3397 was 87 d vs 57 d for IR alone ($P < .0001$; log-rank test). (D) Kaplan-Meier survival curves for mice bearing intracranial GBM12 tumors ($n = 5-6$ mice/group). Median survival for mice treated with IR + PLX3397 was 61 d vs 36 d for IR alone ($P < .0001$; log-rank test).

than U251-luc tumors and therefore mice were divided into the previously described treatment groups at 14 days post-implantation. Median survival of mice bearing intracranial GBM12 tumors treated with IR + PLX3397 was again significantly longer than that for mice treated with IR alone (61 vs 36 d, $P < .0001$; log-rank test) and ~ 3 times longer than median survival of untreated controls (20 d) (Fig. 3D). PLX3397 treatment alone did not have a significant effect on median survival of mice bearing GBM12 tumors. H&E-stained brain sections harvested from IR + PLX3397-treated mice at 48 days indicated that the combined treatment dramatically inhibited tumor growth when compared with brain sections taken from mice in the other treatment groups at earlier time points (Fig. 4A). Although no malignant tissue was evident by H&E stain, staining with a human-specific vimentin antibody did reveal residual tumor cells at the implantation site (Supplementary Fig. S1).

Brain sections taken from U251-luc-implanted mice treated with IR + PLX3397 at 60 days also lacked any detectable hypercellularity associated with proliferating tumor tissue and instead appeared to only have fibrotic regions at the implantation site (Fig. 4B). Importantly, the fibrotic regions were virtually absent of CD11b+ myeloid cells or F4/80+ TAMs, whereas orthotopic tumors treated with IR alone had significantly increased numbers of CD11b+ and F4/80+ cells compared with controls (Fig. 4B and C). To determine whether PLX3397 had any effect on tumor cell proliferation, we

performed an in vitro cell viability assay. PLX3397 did not exhibit cytotoxicity to U251-luc tumor cells but did exhibit cytotoxicity to Raw264.7 macrophages with a lethal dose required to kill 50% of cells of $\sim 6 \mu\text{M}$ (Supplementary Fig. S2).

CSF-1R Inhibition Specifically Depletes CD11b+Ly6c- Monocytes in Irradiated Tumors

In mice, CD11b+ myeloid cells recruited to tumors can be divided into monocytic and granulocytic subpopulations, with the latter being identified by expression of the cell surface antigen Ly6g.¹⁹ FACS analysis of irradiated U251-luc tumors revealed that PLX3397 treatment did not significantly alter the number of Ly6g+ granulocytes in the tumors (Fig. 5A and B). We therefore focused our analysis on Ly6g- monocytes, which can be further divided into 2 subpopulations based on their expression of Ly6c, with Ly6c+ monocytes functioning as precursors to Ly6c- monocytes and TAMs.²⁰⁻²² CSF-1 is the primary growth factor driving monocyte differentiation,⁹ and monocytes isolated from the bone marrow of mice exhibited decreased Ly6c expression when cultured in vitro with recombinant CSF-1 (Supplementary Fig. S3A). Irradiated tumors treated in combination with PLX3397 had significantly fewer CD11b+Ly6c- monocytes (4.5% tumor) than those treated with IR alone (13.0% tumor) (Fig. 5A and C). PLX3397 treatment did not, however, significantly reduce the number of

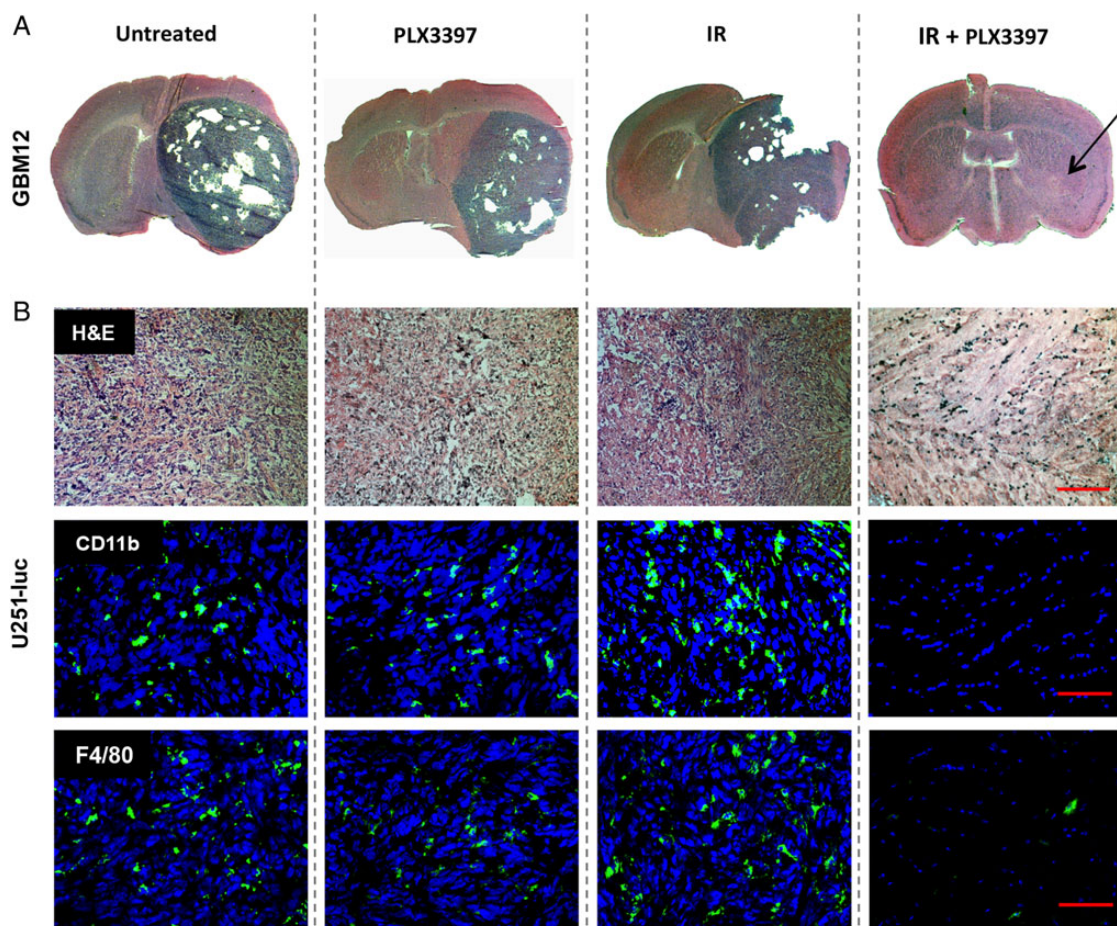


Fig. 4. Immunohistochemistry showing that IR combined with CSF-1R inhibition dramatically inhibits GBM growth. (A) H&E-stained brain sections from mice bearing intracranial GBM12 tumors. Brains were harvested at different time points after implantation: untreated (21 d), PLX3397 (21 d), IR (31 d), and IR + PLX3397 (48 d, arrow indicates implantation site). (B) Serial brain sections from mice bearing intracranial U251-luc tumors harvested at different time points: untreated (43 d), PLX3397 (43 d), IR (57 d), IR + PLX3397 (60 d). Top panels show H&E-stained sections, middle panels show sections stained for CD11b (green), and lower panels show sections stained for F4/80 (green). Scale bar = 200 μ m.

CD11b+Ly6c+ monocytes in irradiated tumors. Interestingly, CSF-1R inhibition caused an increase in the number of CD11b+Ly6c+ cells that was proportional to the reduction in CD11b+Ly6c- cells, suggesting that total numbers of cells in the tumors derived from bone marrow-derived precursors were relatively unchanged (Fig. 5A and C).

CSF-1R Inhibition Blocks Differentiation of Pro-tumorigenic TAMs that Contribute to GBM Recurrence

Alternatively activated (M2) TAMs are known to promote tumorigenesis and refractoriness to radiotherapy^{23,24} and can be identified by expression of CD206 (aka macrophage mannose receptor).²⁵ Immunohistochemical analysis of intracranial U251-luc tumors 7 days after irradiation with 12 Gy revealed that a high proportion of CD11b+ myeloid cells also stained positive for CD206 (Fig. 6A). Tumors treated with IR and PLX3397 had significantly fewer CD206+ macrophages (Fig. 6A). Furthermore, quantitative PCR analysis of myeloid cells isolated from subcutaneous tumors treated with IR and PLX3397 revealed lower expression of genes associated with

an M2 phenotype relative to those treated with IR alone. Myeloid cells from irradiated tumors exhibited increased expression of arginase-1 (*Arg1*), lymphatic vessel endothelial hyaluronic receptor 1 (*Lyve1*), and IL-10 (*Il10*). Expression of *Arg1* and *Il10* was significantly lower in tumors treated with IR + PLX3397, with *Il10* expression reduced to levels lower than in myeloid cells from untreated tumors. Although PLX3397 appeared to slightly inhibit the induction of *Lyve1*, the difference was not statistically significant (Fig. 6B). Conversely, CSF-1R inhibition increased expression of genes associated with a pro-inflammatory M1 TAM phenotype, notably IL-6 (*Il6*), nitric oxide synthase 2 (*Nos2*), and tumor necrosis factor alpha (*Tnfa*). *Il6* was downregulated in TAMs from IR-treated tumors but less downregulated in tumors treated with IR + PLX3397 (Fig. 6C). Nitric oxide synthase 2 (*Nos2*) and tumor necrosis factor alpha (*Tnfa*) were slightly upregulated in TAMs from irradiated tumors but upregulated to a much higher extent (20- to 40-fold) in TAMs from tumors treated with IR + PLX3397 (Fig. 6C).

M2 polarized TAMs are also known to be pro-angiogenic,²⁶ and we have demonstrated that one of the primary mechanisms by which myeloid-derived cells contribute to GBM

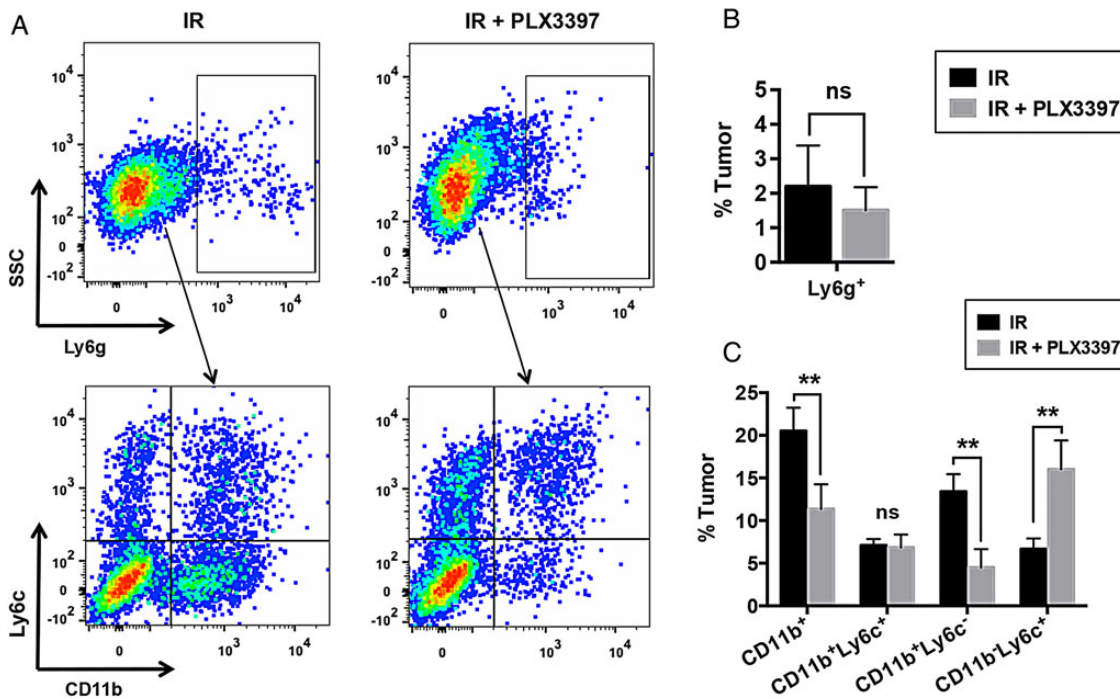


Fig. 5. CSF-1R inhibition specifically depletes CD11b+Ly6c⁻ monocytes in irradiated tumors. Mice bearing subcutaneous U251-luc tumors were treated with IR (12 Gy) ± PLX3397 (40 mg/kg/d). (A) The tumors were harvested 21 d after irradiation and analyzed by FACS using antibodies specific for CD11b, Ly6c, and Ly6g. Gated populations in upper panels indicate Ly6g⁺ cells. Only Ly6g⁻ cells were analyzed for expression of CD11b and Ly6c (lower panels). SSC, side scattered light. (B) Summary of FACS analysis of Ly6g expression. (C) Summary of FACS analysis of CD11b and Ly6c expression. Error bars represent mean ± SEM for $n = 5-6$ mice. ** $P < .01$; Student's t -test.

radioresistance is by promoting the growth of the tumor vasculature.²⁷ Consistent with this, monocytes isolated from the bone marrow of mice that were cultured with CSF-1 exhibited an increased capacity to promote endothelial cell tube formation in vitro (Supplementary Fig. S3B) and upregulated expression of vascular endothelial growth factor (VEGF)A by more than 30-fold (Supplementary Fig. S3C). We therefore analyzed blood vessel formation in subcutaneous U251-luc tumors treated with IR using the pan-endothelial cell marker CD31. At 14 days after IR, PLX3397 reduced CD31+ microvessel density in irradiated tumors by >50% (Supplementary Fig. S3D and S3E). Non-irradiated tumors also showed decreased CD31+ microvessel density relative to untreated controls.

Discussion

The present study suggests that radiotherapy for GBM could be significantly improved by inhibiting CSF-1R signaling in myeloid-derived cells recruited to the irradiated tumors. Using 2 preclinical models, we show that irradiated GBM tumors upregulate expression of the 2 cognate ligands of CSF-1R (CSF-1 and IL-34), recruit increased numbers of CD11b⁺ myeloid cells, and that treatment with the CSF-1R inhibitor PLX3397 prevents myeloid cell recruitment. Further, inhibition of CSF-1R prevents the radiation-induced accumulation of CD11b+Ly6c⁻ monocytes and pro-tumorigenic TAMs that support GBM recurrence. These 2 effects of CSF-1R blockade markedly enhanced radiotherapy for intracranial GBM tumors growing in mice, with the increase

in median survival over controls as much as 2- or 3-fold longer for mice receiving combined treatment than those treated with IR alone.

We and others have previously demonstrated that inhibiting the SDF-1/CXCR4 signaling pathway enhances radiotherapy specifically by blocking CD11b⁺ myeloid cell recruitment to irradiated tumors.^{7,8,28} Recent evidence suggests that inhibiting the CSF-1/CSF-1R pathway represents an alternative strategy to block myeloid cell recruitment to tumors and enhance the effects of radiotherapy or chemotherapy. Xu et al.²⁹ showed that PLX3397 can enhance radiotherapy for prostate carcinomas growing in mice by blocking radiation-induced recruitment of CD11b+F4/80+ TAMs and CD11b+Gr1+ granulocytic myeloid-derived suppressor cells. Similarly, DeNardo et al.³⁰ demonstrated that PLX3397 can potentiate chemotherapy by blocking the recruitment of CD11b+Ly6c⁻F4/80+ TAMs to mammary carcinomas treated with paclitaxel.³⁰ CSF-1 has been reported to be a potent macrophage chemoattractant,^{31,32} and the hypothesis that PLX3397 functions by reducing TAM migration and infiltration into tumors is consistent with the data presented in this report. However, to our knowledge, this is the first report to show that irradiated GBM tumors may upregulate expression of IL-34 in addition to CSF-1.

Since CSF-1 is also the primary growth factor driving differentiation of monocytes into macrophages,⁹ PLX3397 may also function by altering maturation of CD11b+Ly6c⁺ monocytes. PLX3397 did not affect the recruitment of CD11b+Ly6c⁺ immature monocytes to irradiated GBM (Fig. 5) or mammary carcinomas treated with paclitaxel in the aforementioned study.³⁰

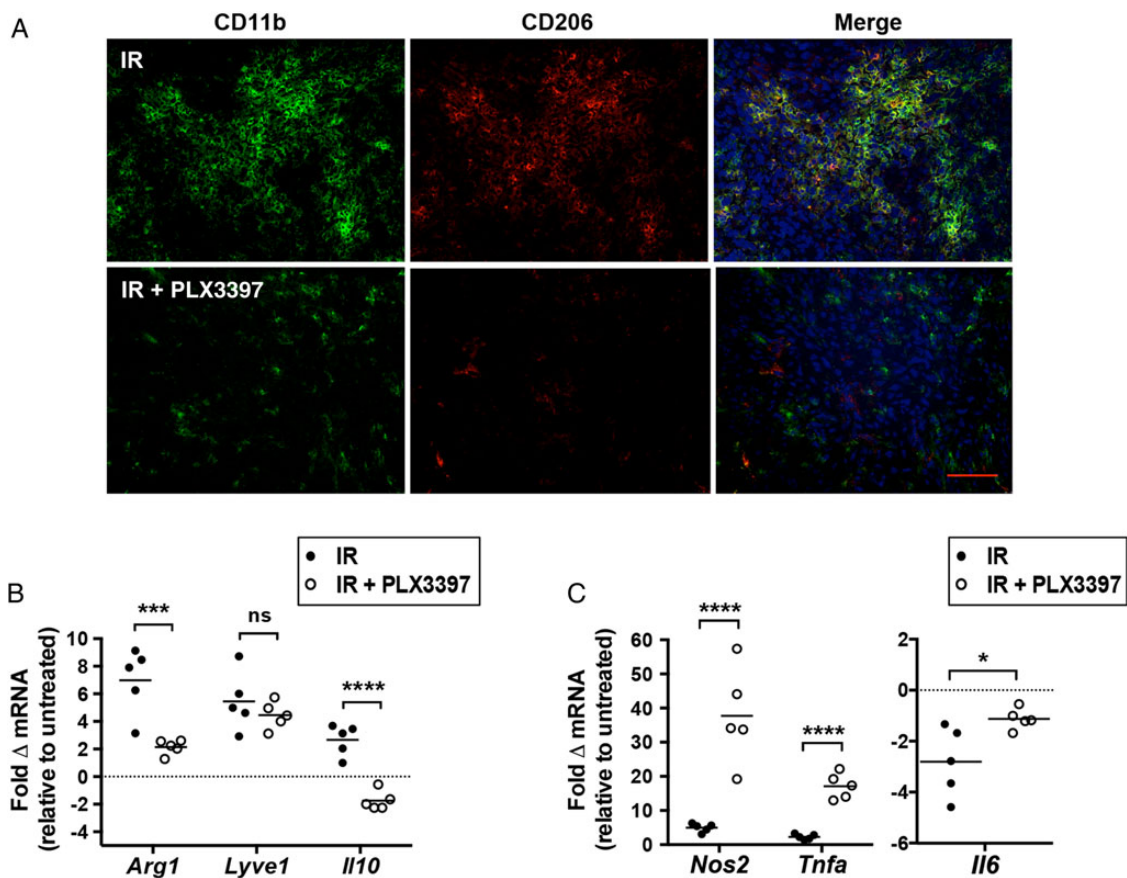


Fig. 6. CSF-1R inhibition specifically blocks differentiation of pro-tumorigenic TAMs that contribute to GBM recurrence after IR. (A) Intracranial U251-luc tumors were assayed for CD206+ macrophages at 7 d after treatment with IR (12 Gy) ± PLX3397 (40 mg/kg/d) by immunohistochemistry. Scale bar = 200 μ m. Myeloid cells isolated from subcutaneous U251-luc tumors 7 d after treatment with IR ± PLX3397 were analyzed for expression of genes associated with M2 (B) and M1 (C) macrophages by quantitative PCR. Expression of each gene indicated was normalized to β -actin expression. Fold change in gene expression is relative to untreated controls; $n = 5$ mice/group. **** $P < .0001$, *** $P < .001$, and * $P < .05$; Student's t -test.

Furthermore, another small molecule inhibitor of CSF-1R, BLZ945, has been shown to inhibit tumor progression in platelet-derived growth factor B-driven glioma (PDG) transgenic mice without altering overall numbers of CD11b+ TAMs.³³ In the PDG model, granulocyte-macrophage colony stimulating factor (GM-CSF) and interferon- γ secreted by the tumor cells promoted survival of TAMs, which instead of being depleted, were “reprogrammed” by BLZ945 to attack the tumor cells. We also observed that PLX3397 does not inhibit IR-induced expression of SDF-1 in GBM tumors growing in mice (unpublished results). Thus, immature monocytes from the bone marrow could be recruited to irradiated GBM tumors via SDF-1 signaling and protected from PLX3397-induced apoptosis by tumor-secreted growth factors.

Altered differentiation of bone marrow-derived monocytes may explain the proportionate increase in CD11b–Ly6c+ cells associated with the reduction in CD11b+Ly6c– mature macrophages in GBM treated with IR and PLX3397. With functional CSF-1 signaling, immature CD11b+Ly6c+ monocytes recruited to irradiated GBM maintain CD11b expression and eventually lose expression of Ly6c as they differentiate into mature TAMs. When CSF-1-mediated differentiation is blocked, Ly6c

expression is maintained and CD11b expression is instead downregulated as monocyte differentiation is commandeered by other cytokines. CSF-1 has been shown to act as a negative regulator of dendritic cell (DC) differentiation,³⁴ and monocytes cultured with GM-CSF and IL-4 in the absence of CSF-1 differentiate into CD11b– DCs.³⁵

Further studies are needed to characterize CD11b–Ly6c+ cells in PLX3397-treated tumors and to determine whether they derive from monocytes recruited from the bone marrow. During inflammation, CD11b+Ly6c+ monocytes can differentiate into macrophages and DCs or remain relatively undifferentiated and act as monocytic myeloid-derived suppressor cells.³⁶ CSF-1 signaling is thought to be essential for the development of pro-tumorigenic M2 macrophages,^{9,37} and we found that PLX3397 treatment decreased the number of M2 macrophages as identified by CD206 expression. Furthermore, the expression of M2-associated genes *Arg1* and *IL10* were significantly lower in TAMs isolated from PLX3397-treated tumors. Meanwhile, *iNOS* and *TNF- α* , genes generally associated with anti-tumorigenic M1 macrophages and DCs,^{24,38} were significantly upregulated. Therefore, the CD11b–Ly6c+ cells detected in PLX3397-treated tumors in this study are likely a combination

of M1 polarized TAMs and monocyte-derived DCs. This reasoning is supported by data showing that TAMs isolated from BLZ945-treated GBM lost their M2 polarization and exhibited enhanced phagocytosis.³³

Several groups have provided compelling evidence that CSF-1R inhibition stimulates antitumor immune responses via activation of CD8+/CD4+ T-cells.^{29,30,33,39-41} However, T-cell activation is unlikely to be the mechanism by which PLX3397 augments IR in our study, since GBM human xenograft models require the use of athymic nude mice that, for the most part, lack adaptive immunity. GBM xenografts treated with IR and PLX3397 exhibited reduced microvessel density, suggesting that inhibition of TAM-mediated angiogenesis in our study is the major mechanism by which CSF-1R inhibition sensitized GBM tumors to irradiation. Human monocytes cultured with CSF-1 have previously been shown to induce VEGF expression and exhibit pro-angiogenic activity,⁴² and we found this to be true for CD11b+Ly6c+ monocytes isolated from the bone marrow of mice. CSF-1–induced monocyte differentiation was also characterized by downregulation of Ly6c expression, demonstrating that a CD11b+Ly6c– phenotype is associated with monocytes that are pro-angiogenic. This corresponds with data showing that Ly6c+ monocytes recruited to tissues by VEGF convert to a Ly6c– phenotype with pro-angiogenic capabilities⁴³ and data showing that Ly6c– monocytes patrol and remodel blood vessels by clearing damaged endothelial cells.^{44,45}

In summary, our findings indicate that disrupting CSF-1R signaling in myeloid-derived cells may be a promising strategy to inhibit GBM recurrence after radiotherapy. Inhibiting CSF-1R with PLX3397 prevented monocytes recruited from the bone marrow from differentiating into TAMs that support tumor growth, and significantly improved GBM response to IR treatment in our preclinical models. Clinical translation of CSF-1R inhibitors and other drugs that target pro-tumorigenic stromal cells may be key to improving the current standard of care and prognosis for human GBM patients.

Supplementary Material

Supplementary material is available online at *Neuro-Oncology* (<http://neuro-oncology.oxfordjournals.org/>).

Funding

This work was supported by grants from the National Institutes of Health (R01 CA149318 and T32 CA09151) and from Plexxikon Inc.

Conflict of interest statement. B.L.K. is an employee of Plexxikon Inc. and J.M.B. is the recipient of a research grant from Plexxikon Inc.

References

- Lim SK, Llaguno SR, McKay RM, et al. Glioblastoma multiforme: a perspective on recent findings in human cancer and mouse models. *BMB Rep*. 2011;44(3):158–164.
- Takano S. Glioblastoma angiogenesis: VEGF resistance solutions and new strategies based on molecular mechanisms of tumor vessel formation. *Brain Tumor Pathol*. 2012;29(2):73–86.
- Hadziahmetovic M, Shirai K, Chakravarti A. Recent advancements in multimodality treatment of gliomas. *Future Oncol*. 2011;7(10):1169–1183.
- Beal K, Abrey L, Gutin P. Antiangiogenic agents in the treatment of recurrent or newly diagnosed glioblastoma: analysis of single-agent and combined modality approaches. *Radiat Oncol*. 2011;6(1):2.
- Chan JL, Lee SW, Fraass BA, et al. Survival and failure patterns of high-grade gliomas after three-dimensional conformal radiotherapy. *J Clin Oncol*. 2002;20(6):1635–1642.
- De Palma M, Lewis Claire E. Macrophage regulation of tumor responses to anticancer therapies. *Cancer Cell*. 2013;23(3):277–286.
- Kioi M, Vogel H, Schultz G, et al. Inhibition of vasculogenesis, but not angiogenesis, prevents the recurrence of glioblastoma after irradiation in mice. *J Clin Invest*. 2010;120(3):694–705.
- Liu S-C, Alomran R, Chernikova SB, et al. Blockade of SDF-1 after irradiation inhibits tumor recurrences of autochthonous brain tumors in rats. *Neurooncol*. 2014;16(1):21–28.
- Pollard JW. Trophic macrophages in development and disease. *Nat Rev Immunol*. 2009;9(4):259–270.
- Gabrilovich DI, Ostrand-Rosenberg S, Bronte V. Coordinated regulation of myeloid cells by tumours. *Nat Rev Immunol*. 2012;12(4):253–268.
- Hume DA, MacDonald KP. Therapeutic applications of macrophage colony-stimulating factor-1 (CSF-1) and antagonists of CSF-1 receptor (CSF-1R) signaling. *Blood*. 2012;119(8):1810–1820.
- Lin EY, Nguyen AV, Russell RG, et al. Colony-stimulating factor 1 promotes progression of mammary tumors to malignancy. *J Exp Med*. 2001;193(6):727–740.
- Pyonteck SM, Gadea BB, Wang HW, et al. Deficiency of the macrophage growth factor CSF-1 disrupts pancreatic neuroendocrine tumor development. *Oncogene*. 2012;31(11):1459–1467.
- Abraham D, Zins K, Sioud M, et al. Stromal cell-derived CSF-1 blockade prolongs xenograft survival of CSF-1-negative neuroblastoma. *Int J Cancer*. 2010;126(6):1339–1352.
- Carlson BL, Pokorny JL, Schroeder MA, et al. Establishment, maintenance and in vitro and in vivo applications of primary human glioblastoma multiforme (GBM) xenograft models for translational biology studies and drug discovery. *Curr Protoc in Pharmacol*. 2011;52:14.16:14.16.1–14.16.23.
- Ozawa T, James CD. Establishing intracranial brain tumor xenografts with subsequent analysis of tumor growth and response to therapy using bioluminescence imaging. *J Vis Exp*. 2010;(41):e1986. doi:10.3791/1986.
- Schmittgen TD, Livak KJ. Analyzing real-time PCR data by the comparative CT method. *Nat Protoc*. 2008;3(6):1101–1108.
- Lin H, Lee E, Hestir K, et al. Discovery of a cytokine and its receptor by functional screening of the extracellular proteome. *Science*. 2008;320(5877):807–811.
- Fleming TJ, Fleming ML, Malek TR. Selective expression of Ly-6G on myeloid lineage cells in mouse bone marrow. RB6-8C5 mAb to granulocyte-differentiation antigen (Gr-1) detects members of the Ly-6 family. *J Immunol*. 1993;151(5):2399–2408.
- Sunderkötter C, Nikolic T, Dillon MJ, et al. Subpopulations of mouse blood monocytes differ in maturation stage and inflammatory response. *J Immunol*. 2004;172(7):4410–4417.
- Movahedi K, Laoui D, Gysemans C, et al. Different tumor microenvironments contain functionally distinct subsets of macrophages derived from Ly6C(high) monocytes. *Cancer Res*. 2010;70(14):5728–5739.

22. Yona S, Kim K-W, Wolf Y, et al. Fate mapping reveals origins and dynamics of monocytes and tissue macrophages under homeostasis. *Immunity*. 2013;38(1):79–91.
23. Quail DF, Joyce JA. Microenvironmental regulation of tumor progression and metastasis. *Nat Med*. 2013;19(11):1423–1437.
24. Biswas SK, Mantovani A. Macrophage plasticity and interaction with lymphocyte subsets: cancer as a paradigm. *Nat Immunol*. 2010;11(10):889–896.
25. Mantovani A, Sica A, Sozzani S, et al. The chemokine system in diverse forms of macrophage activation and polarization. *Trends Immunol*. 2004;25(12):677–686.
26. Mantovani A, Biswas SK, Galdiero MR, et al. Macrophage plasticity and polarization in tissue repair and remodelling. *J Pathol*. 2013;229(2):176–185.
27. Russell JS, Brown JM. The irradiated tumor microenvironment: role of tumor-associated macrophages in vascular recovery. *Front in Physiol*. 2014;(13). doi: 10.1186/1476-4598-13-177.
28. Kozin SV, Kamoun WS, Huang Y, et al. Recruitment of myeloid but not endothelial precursor cells facilitates tumor regrowth after local irradiation. *Cancer Res*. 2010;70(14):5679–5685.
29. Xu J, Escamilla J, Mok S, et al. CSF1R signaling blockade stanches tumor-infiltrating myeloid cells and improves the efficacy of radiotherapy in prostate cancer. *Cancer Res*. 2013;73(9):2782–2794.
30. DeNardo DG, Brennan DJ, Rexhepaj E, et al. Leukocyte complexity predicts breast cancer survival and functionally regulates response to chemotherapy. *Cancer Discov*. 2011;1:54–67.
31. Wang JM, Griffin JD, Rambaldi A, et al. Induction of monocyte migration by recombinant macrophage colony-stimulating factor. *J Immunol*. 1988;141(2):575–579.
32. Webb SE, Pollard JW, Jones GE. Direct observation and quantification of macrophage chemoattraction to the growth factor CSF-1. *J Cell Sci*. 1996;109(4):793–803.
33. Pyonteck SM, Akkari L, Schuhmacher AJ, et al. CSF-1R inhibition alters macrophage polarization and blocks glioma progression. *Nat Med*. 2013;19(10):1264–1272.
34. León B, López-Bravo M, Ardavin C. Monocyte-derived dendritic cells. *Semin Immunol*. 2005;17(4):313–318.
35. León B, Martínez del Hoyo G, Parrillas V, et al. Dendritic cell differentiation potential of mouse monocytes: monocytes represent immediate precursors of CD8– and CD8+ splenic dendritic cells. *Blood*. 2004;103(7):2668–2676.
36. Geissmann F, Manz MG, Jung S, et al. Development of monocytes, macrophages, and dendritic cells. *Science*. 2010;327(5966):656–661.
37. Martinez FO, Gordon S, Locati M, et al. Transcriptional profiling of the human monocyte-to-macrophage differentiation and polarization: new molecules and patterns of gene expression. *J Immunol*. 2006;177(10):7303–7311.
38. Hashimoto D, Miller J, Merad M. Dendritic cell and macrophage heterogeneity in vivo. *Immunity*. 2011;35(3):323–335.
39. Zhu Y, Knolhoff BL, Meyer MA, et al. CSF1/CSF1R blockade reprograms tumor-infiltrating macrophages and improves response to T-cell checkpoint immunotherapy in pancreatic cancer models. *Cancer Res*. 2014;74(18):5057–5069.
40. Mok S, Koya RC, Tsui C, et al. Inhibition of CSF-1 receptor improves the antitumor efficacy of adoptive cell transfer immunotherapy. *Cancer Res*. 2014;74(1):153–161.
41. Priceman SJ, Sung JL, Shaposhnik Z, et al. Targeting distinct tumor-infiltrating myeloid cells by inhibiting CSF-1 receptor: combating tumor evasion of antiangiogenic therapy. *Blood*. 2010;115(7):1461–1471.
42. Eubank TD, Galloway M, Montague CM, et al. M-CSF Induces vascular endothelial growth factor production and angiogenic activity from human monocytes. *J Immunol*. 2003;171(5):2637–2643.
43. Avraham-Davidi I, Yona S, Grunewald M, et al. On-site education of VEGF-recruited monocytes improves their performance as angiogenic and arteriogenic accessory cells. *J Exp Med*. 2013;210(12):2611–2625.
44. Auffray C, Fogg D, Garfa M, et al. Monitoring of blood vessels and tissues by a population of monocytes with patrolling behavior. *Science*. 2007;317(5838):666–670.
45. Carlin Leo M, Stamatiades Efstathios G, Auffray C, et al. Nr4a1-dependent Ly6C low monocytes monitor endothelial cells and orchestrate their disposal. *Cell*. 2013;153(2):362–375.